Published March 23, 2009

Akt regulates L-type Ca^{2+} channel activity by modulating $Ca_v\alpha1$ protein stability

Daniele Catalucci,[1,3] Deng-Hong Zhang,[1] Jaime DeSantiago,[4,5] Franck Aimond,[6] Guillaume Barbara,[7] Jean Chemin,[7] Désiré Bonci,[8] Eckard Picht,[4,5] Francesca Rusconi,[3] Nancy D. Dalton,[1] Kirk L. Peterson,[1] Sylvain Richard,[6] Donald M. Bers,[4,5] Joan Heller Brown,[2] and Gianluigi Condorelli[1,3]

[1]Division of Cardiology, Department of Medicine and [2]Department of Pharmacology, University of California, San Diego, La Jolla, CA 92093
[3]Istituto di Ricovero e Cura a Carattere Scientifico Multimedica, Milan 20138, Italy
[4]Department of Pharmacology, School of Medicine and [5]Genome and Biomedical Sciences Facility, University of California, Davis, Davis, CA 95616
[6]Physiopathologie Cardiovasculaire, Institut National de la Santé et de la Recherche Médicale Unité 637, Université Montpellier 1, Montpellier 34295, France
[7]Département de Physiologie, Institut de Génomique Fonctionnelle, Centre National de la Recherche Scientifique Unité Mixte de Recherche 5203, Institut National de la Santé et de la Recherche Médicale Unité 661, Université Montpellier 2, Montpellier 34295, France
[8]Dipartimento di Ematologia, Oncologia e Medicina Molecolare, Istituto Superiore Sanità, Rome 00161, Italy

The insulin IGF-1–PI3K–Akt signaling pathway has been suggested to improve cardiac inotropism and increase Ca^{2+} handling through the effects of the protein kinase Akt. However, the underlying molecular mechanisms remain largely unknown. In this study, we provide evidence for an unanticipated regulatory function of Akt controlling L-type Ca^{2+} channel (LTCC) protein density. The pore-forming channel subunit $Ca_v\alpha1$ contains highly conserved PEST sequences (signals for rapid protein degradation), and in-frame deletion of these PEST sequences results in increased $Ca_v\alpha1$ protein levels. Our findings show that Akt-dependent phosphorylation of $Ca_v\beta2$, the LTCC chaperone for $Ca_v\alpha1$, antagonizes $Ca_v\alpha1$ protein degradation by preventing $Ca_v\alpha1$ PEST sequence recognition, leading to increased LTCC density and the consequent modulation of Ca^{2+} channel function. This novel mechanism by which Akt modulates LTCC stability could profoundly influence cardiac myocyte Ca^{2+} entry, Ca^{2+} handling, and contractility.

Introduction

The IGF-1 (insulin growth factor 1)–PI3K (phosphatidylinositol 3-kinase)–Akt pathway plays a crucial role in a broad range of biological processes involved in the modulation of local responses as well as processes implicated in metabolism, cell proliferation, transcription, translation, apoptosis, and growth. In the heart, the IGF-1–PI3K–Akt pathway is involved in the regulation of contractile function, and impairment of this signaling pathway is considered an important determinant of cardiac function (Condorelli et al., 2002; McMullen et al., 2003; Ceci et al., 2004; McMullen et al., 2004; Catalucci and Condorelli, 2006; Sun et al., 2006).

The Akt (also called PKB) family of Ser/Thr kinases consists of three isoforms (Akt-1, -2, and -3) that are activated by IGF-1 and insulin through PI3K, which is a member of the lipid kinase family involved in the phosphorylation of membrane phosphoinositides (Ceci et al., 2004). The product of PI3K binds to the pleckstrin domain of Akt and induces its translocation from the cytosol to the plasma membrane, where Akt becomes accessible for phosphorylation by PDK1 (phosphoinositide-dependent kinase 1), resulting in its activation (Ceci et al., 2004; Bayascas et al., 2008). The Ca^{2+} current ($I_{Ca,L}$) in both cardiomyocytes and neuronal cells has been shown to be increased by Akt activation (Blair et al., 1999; Viard et al., 2004; Catalucci and Condorelli, 2006; Sun et al., 2006) and decreased by Akt inhibition (Viard et al., 2004; Catalucci and Condorelli, 2006; Sun et al., 2006), suggesting a pivotal role of Akt in regulating L-type Ca^{2+} channel (LTCC) complex function.

D. Catalucci and D.-H. Zhang contributed equally to this paper.

Correspondence to Daniele Catalucci: daniele.catalucci@itb.cnr.it; or Gianluigi Condorelli: gcondorelli@ucsd.edu

Abbreviations used in this paper: AID, α1-interacting domain; ANOVA, analysis of variance; DN, dominant-negative; GAPDH, glyceraldehyde-3-phosphate dehydrogenase; KO, knockout; LTCC, L-type Ca^{2+} channel; PLN, phospholamban; Ryr, ryanodine receptor; siAkt, small interfering Akt; SR, sarcoplasmic reticulum; TEA, tetraethylammonium; Tg, transgenic; WT, wild type.

Supplemental Material can be found at:
http://jcb.rupress.org/content/suppl/2009/03/21/jcb.200805063.DC1.html

The Rockefeller University Press $30.00
J. Cell Biol. Vol. 184 No. 6 923–933
www.jcb.org/cgi/doi/10.1083/jcb.200805063

Published March 23, 2009

In cardiomyocytes, the LTCC is composed of different subunits: the pore-forming subunit $Ca_v\alpha1$ and the accessory β and α2δ subunits (Catterall, 2000; Bourinet et al., 2004). The opening of the LTCC is primarily regulated by the membrane potential and by other factors, including a variety of hormones, protein kinases, phosphatases, and accessory proteins (Bodi et al., 2005). In healthy cardiomyocytes, electrical excitation starting during the upstroke of the action potential leads to cytosolic Ca^{2+} influx through opening of the LTCC (Bers and Perez-Reyes, 1999; Richard et al., 2006). This triggers the CICR (Ca-induced Ca release) of intracellular Ca^{2+} from the sarcoplasmic reticulum (SR) through activation of the ryanodine receptor (Ryr), eventually leading to cardiomyocyte contraction (Bers, 2002).

The importance and ubiquity of Ca^{2+} as an intracellular signaling molecule suggests that altered channel function could give rise to widespread cellular and organ defects. Indeed, a variety of cardiovascular diseases, including atrial fibrillation, heart failure, ischemic heart disease, Timothy syndrome, and diabetic cardiomyopathy, have been related to alterations in the density or function of the LTCC (Mukherjee and Spinale, 1998; Quignard et al., 2001; Bodi et al., 2005; Pereira et al., 2006). However, the molecular basis for dysregulation of LTCC function and the possible involvement of Akt in $I_{Ca,L}$ regulation remain unresolved.

Recently, a seminal study in neuronal cells revealed the importance of Akt-dependent phosphorylation of the $Ca_v\beta2$ subunit in promoting the chaperoning of the $Ca_v2.2$ pore-forming unit to the plasma membrane (Viard et al., 2004). In this study, we identify a novel posttranslational mechanism by which Akt modulates LTCC function under physiological conditions, highlighting the pivotal role of this kinase in cardiac function. Interestingly, our results show that the pore-forming channel subunit $Ca_v\alpha1$ contains highly conserved PEST sequences that direct rapid protein degradation and demonstrate that Akt-mediated phosphorylation of the $Ca_v\beta2$ LTCC chaperone subunit prevents PEST site recognition, thereby slowing or preventing $Ca_v\alpha1$ degradation. This mechanism of action might be an essential process for Ca^{2+} channel functional regulation, thus contributing to normal or better cardiomyocyte contractile function.

Results

To gain insight into the mechanism of action by which Akt regulates $I_{Ca,L}$ and Ca^{2+} handling in the heart, we studied a mouse line with tamoxifen-inducible (Sohal et al., 2001) and cardiac-specific deletion of PDK1, the upstream activator of all three Akt isoforms. Mice in which exons 3 and 4 of the *pdk1* gene were flanked by *loxP* excision sequences (Lawlor et al., 2002) were crossed with transgenic (Tg) mice expressing an inducible and cardiac-specific MerCreMer α-MHC promoter driving the *cre* recombinase gene (Sohal et al., 2001), resulting in MerCreMer α-MHC PDK1 mice (knockout [KO]). As opposed to the previously described muscle creatine kinase–Cre PDK1 mouse model (Mora et al., 2003) in which PDK1 is embryonically deleted in all striated muscles, this model allows for specific deletion of PDK1 in the adult heart. A further advantage of this model is the inducible cardiac-specific deletion that was necessary to circumvent the embryonic lethality we observed in a mouse model with constitutive α-MHC–Cre cardiac deletion of PDK1 (unpublished data). Similar to the muscle creatine kinase–Cre PDK1 mouse model (Lawlor et al., 2002), PDK1 gene deletion in the adult mouse heart (KO; Fig. S1, A and B) resulted in a lethal phenotype with a mortality that reached 100% at 10 d after tamoxifen injection (Fig. S1 C). Age-matched littermate control mice without *cre* (wild type [WT]) were unaffected by tamoxifen treatment. Consistent with findings from the previously reported analysis of the PDK1 KO mouse model (Lawlor et al., 2002), cardiac function evaluated by echocardiography at 7 d after tamoxifen injection revealed dramatically impaired systolic function with severe dilated cardiomyopathy and an abrupt drop in fractional shortening in KO but not in WT mice (Fig. S1 D, Table S1, and not depicted). Histological examination substantiated the echocardiographic findings, revealing dilatation of both ventricles and atria (Fig. S1 E) with apparently no evidence of significant apoptosis or interstitial fibrosis (Fig. S1, F and G). These observations indicate that PDK1/Akt activity plays a major role in maintaining adult heart function.

Deficiency in Akt activity leads to a reduction in the $Ca_v\alpha1$ protein level

Using the cardiac-specific PDK1 KO mouse model, we investigated whether deficiency in Akt activity affects the expression or activation of signaling molecules that are implicated in Ca^{2+} handling and cardiac function. A time course analysis of extracts from WT and KO mouse ventricles revealed striking changes in protein expression upon induction of the PDK1 KO (Fig. 1, A and B). Notably, KO mice had decreased protein levels of the pore-forming Ca^{2+} channel subunit, $Ca_v\alpha1$, which progressed as PDK1 protein expression gradually declined. No change in the protein level of the regulatory $Ca_v\beta2$ subunit was observed. As PDK1 expression decayed, levels of Akt activation also dramatically decreased (assessed by phosphorylation of Akt at the PDK1 phosphorylation site Thr308) despite unaltered expression of total Akt protein (Fig. 1, A and B). Furthermore, Akt activity (assessed using GSK-3β as a substrate) was virtually absent in KO hearts (Fig. 1 C). Based on this evidence, we decided to perform further experiments at day 6 after the beginning of treatment.

Although the main physiological action of PDK1 is on Akt activation, PDK1 can potentially influence other members of the cAMP-dependent, cGMP-dependent, and PKC (AGC) kinase protein family such as PKC and PKA, which could also affect cellular Ca^{2+} handling (Williams et al., 2000; Mora et al., 2004). However, PKC activity was unchanged in KO mice (1.15 ± 0.05–fold greater than WT; not statistically significant; assessed by an assay using a PKC-specific peptide as substrate). There was no apparent effect of PDK1 deletion on SERCA2a (Fig. S2 A) as well as PKA activity because the phosphorylation of specific PKA regulatory sites in two SR Ca^{2+} regulatory proteins, Ryr (Ryr2-P2809) and phospholamban (PLN; PLN-P16), were unchanged in KO mice (Fig. S2 B), although it cannot be

Published March 23, 2009

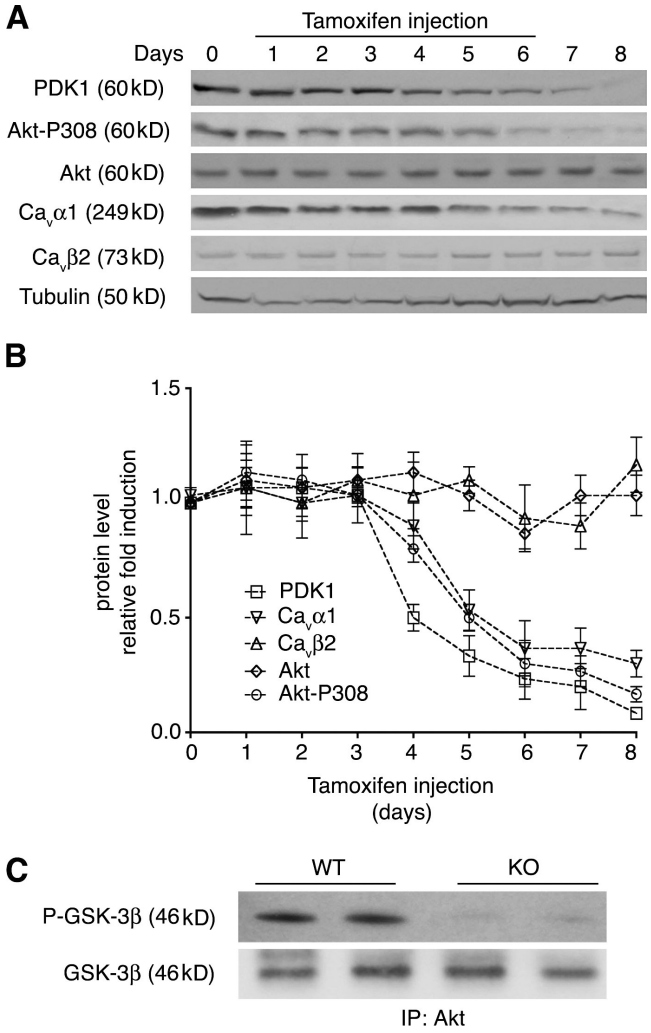

Figure 1. **Alteration of Ca^{2+} handling proteins in PDK1 KO cardiomyocytes.** (A and B) Western blot (A) and densitometric (B) analyses of ventricular homogenates along a time course of tamoxifen inductions (day 1–6 treatment is indicated by the line in A) using various antibodies. A representative experiment is shown ($n = 3$). Error bars show SD. (C) Total Akt activity in WT and KO cardiomyocyte lysates assayed using a GSK-3β/α Akt-specific substrate. IP, immunoprecipitation.

excluded that typical changes associated with heart failure and secondary to adrenergic receptor hyperactivation may take place at subsequent time points. Collectively, these data suggest that an acute reduction in Akt activation affects expression of proteins involved in the Ca^{2+} influx into the cell.

Deficiency in Akt activity affects $I_{Ca,L}$

Ca^{2+} handling and inotropism were examined in adult cardiomyocytes freshly isolated from WT and KO mice. Using the whole cell voltage-clamp technique, we recorded and analyzed LTCC $I_{Ca,L}$ properties. No difference in cell size was observed between WT and KO cells as deduced from membrane capacitance measurements. Membrane capacitance was 116 ± 6 pF in WT cells ($n = 18$) and 115 ± 6 pF in KO cells ($n = 18$). However, the density of $I_{Ca,L}$ (picoampere/picofarad) was decreased in KO versus WT (Fig. 2 B). At 0 mV, the density of $I_{Ca,L}$ was −9.08 ± 0.96 pA/pF in KO cells ($n = 12$) versus −16.26 ± 0.96 pA/pF in WT cells ($n = 12$; $P < 0.001$). In addition, there was no significant difference in either steady-state activation or inactivation curves (unpublished data). Indeed, mean half-activation occurred at −12.97 ± 0.53 mV in WT cells versus −15.07 ± 0.66 mV in KO cells, and mean half-inactivation occurred at −31.11 ± 0.48 mV in WT cells versus −30.77 ± 0.42 mV in KO cells. The absence of a shift in the voltage dependence of these properties (Fig. 2 B) was consistent with the absence of modification in gating properties of the LTCC, suggesting that a reduction in the number of functional LTCCs can account for the observed decrease in $I_{Ca,L}$ in KO mice. Of note, the decay kinetics of $I_{Ca,L}$ were slower in KO cells compared with WT cells with a decrease in the early fast inactivating component (Fig. 2 A). Consistent with previous observations by us and others regarding the role of Akt in cardiac function (Blair et al., 1999; Condorelli et al., 2002; Kim et al., 2003; Sun et al., 2006), both contraction (Fig. 2 C) and systolic Ca^{2+} amplitudes (Ca^{2+} transients; Fig. 2 D and Fig. S3 A) were significantly depressed (by ∼35% and 30%, respectively; $P < 0.05$) in KO cardiomyocytes compared with WT littermates.

The observed reduction in Ca^{2+} transient amplitude and cardiac contractility could be explained by reduced Ca^{2+} entry into cells via the LTCC, but decreased intracellular Ca^{2+} release from the SR may also contribute. However, although the Ca^{2+} transient amplitude between the systolic and diastolic phase (twitch) was smaller in KO cardiomyocytes (Fig. S3 B, left bars), no difference in total SR Ca^{2+} content was found (Fig. S3 B, right bars), suggesting that the decrease in Ca^{2+} transient amplitude is only caused by reduced Ca^{2+} entry. This is consistent with the observed slowing of the early fast inactivation of $I_{Ca,L}$ (Fig. 2 A), which is highly dependent on CICR-triggered SR Ca^{2+} release during the action potential (Richard et al., 2006). Therefore, we conclude that the reduced $I_{Ca,L}$ may contribute to the reduced contractility in KO hearts.

Akt regulates the $Ca_v\alpha1$ protein level at the plasma membrane

The properties of the $Ca_v\alpha1$ subunit are known to be markedly affected by LTCC accessory subunits (Catterall, 2000; Bourinet et al., 2004). Among the LTCC accessory subunits expressed in the heart, $Ca_v\beta2$ is known to act as a chaperone for the $Ca_v\alpha1$ subunit, both as a positive modulator of channel opening probability and for its trafficking from the ER to the plasma membrane (Yamaguchi et al., 1998; Viard et al., 2004). Therefore, supported by previous results (Viard et al., 2004) as well as corroborated by unchanged $Ca_v\alpha1$ mRNA levels in KO compared with WT hearts (Fig. 3 A), we hypothesized that in the heart, an Akt-mediated phosphorylation of the LTCC accessory subunit would mainly affect trafficking of $Ca_v\alpha1$ protein to the plasma membrane. However, because the amount of $Ca_v\alpha1$ was reduced in both microsomal and membrane fractions from KO extracts compared with WT (Fig. 3 B), we hypothesized that the reduced $Ca_v\alpha1$ level observed in KO mice was caused by enhanced protein degradation in addition to impaired protein translocation to the plasma membrane. To assess the pathway involved in the Akt-dependent $Ca_v\alpha1$ protein degradation, three sets of specific cell degradation system inhibitors were examined for their ability to

Published March 23, 2009

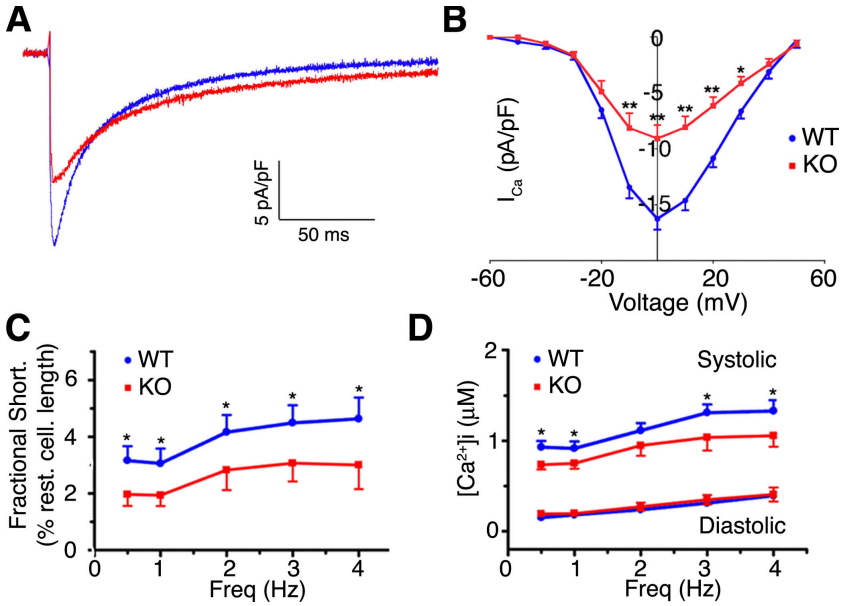

Figure 2. **Impaired intracellular Ca^{2+} handling and contractility in PDK1 KO cardiomyocytes.** (A and B) Smaller Ca^{2+} current in KO cardiomyocytes. (A) Whole cell representative $I_{Ca,L}$ currents normalized for difference in cell size. (B) $I_{Ca,L}$ I-V current/voltage relationships (n = 12; *, $P < 0.05$; **, $P < 0.01$). (C and D) Cardiomyocyte contraction and Ca^{2+} transients at different stimulation frequencies. (C) Cardiomyocyte shortening is decreased in KO compared with WT cardiomyocytes (*, $P < 0.05$; ANOVA). (D) Ca^{2+} frequency relationship indicates smaller peak systolic but not diastolic Ca^{2+} in KO compared with WT cells (*, $P < 0.05$; ANOVA). Error bars show SEM.

prevent the decrease in $Ca_v\alpha1$ protein elicited by Akt inhibition. Treatment of $Ca_v\alpha1$- and $Ca_v\beta2$-cotransfected cells with bafilomycin-A1, an inhibitor of the lysosomal degradation system responsible for the degradation of many membrane proteins (Dice, 1987), prevented the decrease in $Ca_v\alpha1$ protein induced by Akt inhibition (Fig. 3 C, top). Conversely, a ubiquitin/proteasome inhibitor, MG132, failed to protect $Ca_v\alpha1$ from protein degradation. Similar results were obtained by inhibiting calpain, the intracellular Ca^{2+}-dependent Cys protease known to be involved in membrane protein degradation (Belles et al., 1988; Romanin et al., 1991). Intriguingly, the bafilomycin-A1–dependent protection effect was abolished in the absence of $Ca_v\beta2$ cotransfection, a condition under which $Ca_v\alpha1$ is retained in the ER (Fig. 3 C, bottom). All together, these results confirm that Akt activity is regulating $Ca_v\alpha1$ protein density and reveal that in the absence of Akt function, $Ca_v\alpha1$ is susceptible to lysosome-mediated membrane protein degradation.

Because $Ca_v\beta2$ is the only LTCC accessory subunit containing an Akt phosphorylation consensus site (Viard et al., 2004), we hypothesized that $Ca_v\alpha1$ protein degradation at the plasma membrane might result from loss of $Ca_v\beta2$ chaperone activity in the absence of Akt-induced phosphorylation. In support

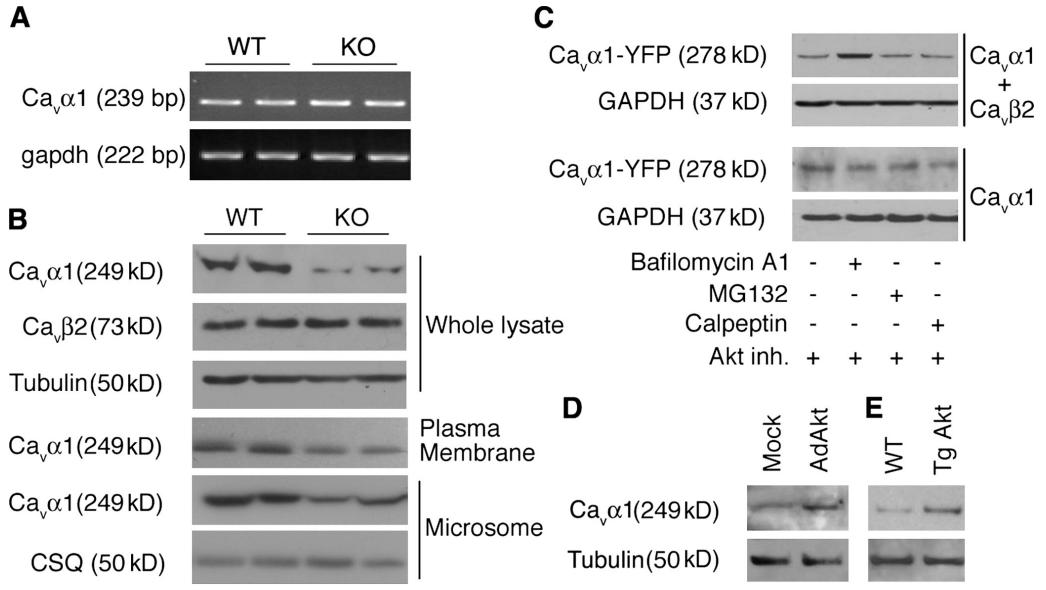

Figure 3. **Akt mediates regulation of $Ca_v\alpha1$ protein density at the plasma membrane.** (A) RT-PCR analysis of $Ca_v\alpha1$ mRNA expression from WT and KO ventricular extracts. GAPDH served as a loading control. (B) Western blot analysis of whole lysate, membrane, and microsomal fractions from WT and KO ventricular extracts. CSQ, calsequestrin. (C) YFP-$Ca_v\alpha1$–transfected COS-7 cells alone or in combination with $Ca_v\beta2$ expression vector were serum starved and treated with Akt inhibitor (Akt inh.) and 1 μM bafilomycin-A1, 25 μM MG132, or 25 μM calpeptin. 6 h after drug administration, cell lysates were prepared and subjected to Western blot analysis for YFP. GAPDH served as a loading control. (D and E) $Ca_v\alpha1$ protein levels in KO cardiomyocytes infected with empty (mock) or active E40K-Akt (AdAkt)–expressing adenoviral vector (D) and in whole lysates of WT and E40K-Akt (Tg Akt) hearts (E). Representative experiments are shown (n = 4).

Published March 23, 2009

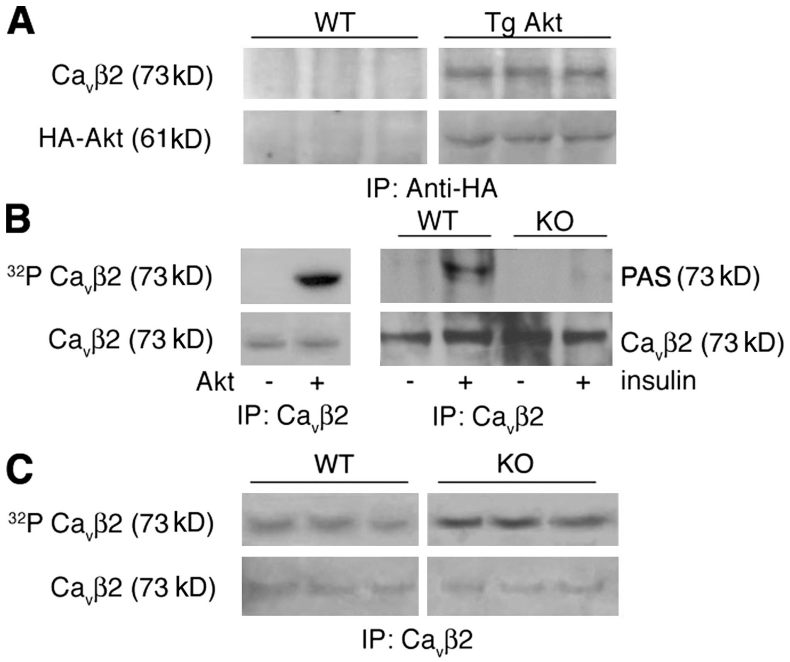

Figure 4. **Akt interacts with and phosphorylates $Ca_v\beta2$.** (A) Coimmunoprecipitation assay of Akt and $Ca_v\beta2$. Ventricular homogenates from WT and HA–E40K-Akt Tg mice (Tg Akt) immunoprecipitated with antibodies against HA and immunoblotted for $Ca_v\beta2$ as well as HA as a control. (B) Examination of $Ca_v\beta2$ phosphorylation by Akt. In vitro kinase assays were performed with immunoprecipitated $Ca_v\beta2$ incubated with recombinant active Akt and ^{32}P-labeled ATP (left) or immunoprecipitated $Ca_v\beta2$ from WT and KO cardiac extracts from mice treated or not treated with 1 mU/g insulin using phospho-Akt substrate (PAS) antibody (right). (C) Back phosphorylation assay of $Ca_v\beta2$ from WT and KO hearts. Immunoprecipitated $Ca_v\beta2$ from solubilized membranes was in vitro back phosphorylated using recombinant active Akt and [γ^{32}]ATP. Precipitate amounts were assayed for [^{32}P]$Ca_v\beta2$ and total $Ca_v\beta2$. Representative experiments are shown (n = 4). IP, immunoprecipitation.

of this hypothesis, forced expression of the active E40K-Akt mutant (AdAkt) restored $Ca_v\alpha1$ protein levels in isolated cardiomyocytes from KO mice (Fig. 3 D). Similarly, cardiomyocytes from Tg mice expressing constitutively active HA–E40K-Akt (Tg Akt; Condorelli et al., 2002) showed increased $Ca_v\alpha1$ levels compared with WT controls (Fig. 3 E).

Akt is a determinant for $Ca_v\alpha1$ protein level regulation by direct phosphorylation of the $Ca_v\beta2$ chaperone subunit

To assess whether Akt is directly involved in modulation of $Ca_v\beta2$ chaperone activity in the heart, we first confirmed the interaction between Akt and $Ca_v\beta2$. Ventricular homogenates derived from either WT or Tg Akt mice were immunoprecipitated with anti-HA antibody and assayed for $Ca_v\beta2$, which revealed association of the $Ca_v\beta2$ subunit with active Akt (Fig. 4 A). Similarly, $Ca_v\beta2$ was found to coimmunoprecipitate with insulin-stimulated endogenous Akts (Fig. S4 A).

To determine whether $Ca_v\beta2$ can be phosphorylated by Akt, $Ca_v\beta2$ immunoprecipitates from cardiac homogenates were incubated with recombinant active Akt and γ-[^{32}P]ATP. A band corresponding to phosphorylated $Ca_v\beta2$ was detected only in the presence of the kinase (Fig. 4 B, left). To determine whether the $Ca_v\beta2$ subunit was phosphorylated by Akt in vivo, we treated overnight-starved mice with 1 mU/g insulin to induce activation of Akt (Bayascas et al., 2008). 20 min after treatment, $Ca_v\beta2$ was immunoprecipitated from ventricular homogenates, subjected to Western blot analysis, and probed for phosphorylated Akt consensus sites using phospho-Akt substrate antibody. This revealed insulin-stimulated phosphorylation of $Ca_v\beta2$ in WT but not in KO hearts (Fig. 4 B, right). Furthermore, a back phosphorylation assay, which is used to assess the basal state of $Ca_v\beta2$ phosphorylation, revealed a reduction of the basal phosphorylation level of $Ca_v\beta2$ by 36% ($P < 0.05$) in KO mouse ventricle compared with WT (Fig. 4 C). Collectively, these data demonstrate that active Akt binds to and phosphorylates $Ca_v\beta2$, the chaperone for $Ca_v\alpha1$.

To directly assess whether Akt phosphorylation of $Ca_v\beta2$ protects $Ca_v\alpha1$ from protein degradation, we constructed a mutant of $Ca_v\beta2$ in which Ser625, which is contained in the putative Akt consensus site (R-X-X-R-S/T), was replaced by glutamate ($Ca_v\beta2$-SE) to mimic phosphorylation. Cotransfection of 293T cells with $Ca_v\alpha1$ and $Ca_v\beta2$-SE resulted in $Ca_v\alpha1$ protein levels that were increased compared with those found when cotransfected with $Ca_v\beta2$-WT (Fig. 5 A). Similarly, $Ca_v\alpha1$ expression was increased in insulin-treated $Ca_v\beta2$-WT–cotransfected cells (Fig. 5 A). Notably, the active phosphomimic $Ca_v\beta2$-SE also counteracted the down-regulation of $Ca_v\alpha1$ induced by an Akt inhibitor (Fig. 5 B). Opposite results were obtained with a dominant-negative (DN) $Ca_v\beta2$ mutant in which Ser was replaced by Ala ($Ca_v\beta2$-SA) to prevent Akt phosphorylation. Indeed, $Ca_v\alpha1$ protein levels were reduced when coexpressed with $Ca_v\beta2$-SA (Fig. 5 C). In addition, insulin stimulation failed to increase $Ca_v\alpha1$ in the presence of the DN $Ca_v\beta2$-SA mutant (Fig. 5 C). Consistent with the hypothesis that $Ca_v\alpha1$ protein down-regulation relies on Akt kinase activity, overexpression of a DN form of Akt (AdAktDN) resulted in a significant reduction in $Ca_v\alpha1$ protein levels, whereas forced expression of AdAkt was sufficient to counteract $Ca_v\alpha1$ reduction in a serum-free condition, in which Akt is not phosphorylated (Fig. S4 B). Furthermore, suppression of Akt expression in 293T cells by siRNA (small interfering Akt [siAkt]) resulted in reduction of the $Ca_v\alpha1$ protein level (Fig. 5 D).

To support the evidence that Akt-dependent phosphorylation of $Ca_v\beta2$ is a determinant for $Ca_v\alpha1$ stability and functionality, we measured the effect of the $Ca_v\beta2$ mutants on Ca^{2+} current. Although cotransfection of cells with $Ca_v\alpha1$ and $Ca_v\beta2$-WT resulted in significant depressed $I_{Ca,L}$ in serum-free medium compared with serum-containing medium in which Akt is phosphorylated (not depicted), cotransfection of $Ca_v\alpha1$

Published March 23, 2009

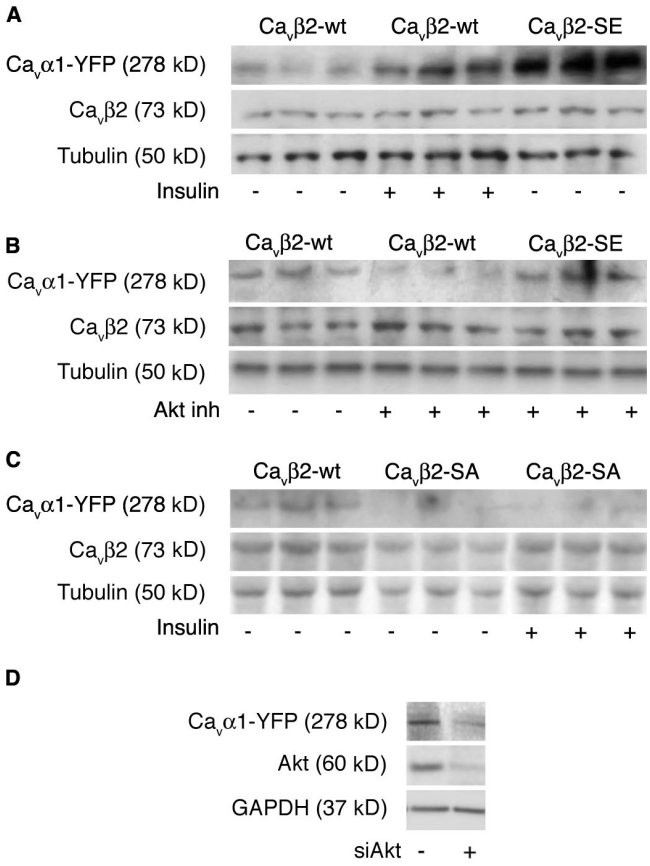

Figure 5. **Akt phosphorylation of $Ca_v\beta2$ protects $Ca_v\alpha1$ from protein degradation.** (A–C) YFP-$Ca_v\alpha1$–cotransfected 293T cells with the indicated mutant variant of $Ca_v\beta2$. Cells were serum starved overnight and treated with 100 µM insulin (A and C) or 5 µM Akt inhibitor (Akt inh; B) as indicated. The expression of YFP-$Ca_v\alpha1$ in lysates was monitored by Western blot analysis with anti-YFP antibody and normalized based on transfection efficiency ($Ca_v\beta2$) and protein amount (tubulin; $n = 3$). (D) $Ca_v\alpha1$- and $Ca_v\beta2$-cotransfected 293T cells were treated with siAkt-expressing vector as indicated. 3 d after transfection, cell lysate was tested by Western blot analysis. Protein loading was normalized to GAPDH levels. Representative experiments are shown ($n = 3$).

and $Ca_v\beta2$-SE mutant but not $Ca_v\beta2$-SA mutant completely counteracted this reduction (Fig. 6).

Akt regulates $Ca_v\alpha1$ protein stability

PEST sequences have been suggested to serve as signals for rapid proteolytic degradation through the cell quality control system (Rechsteiner, 1990; Smith et al., 1993; Krappmann et al., 1996; Sandoval et al., 2006). Notably, PEST-mediated protein degradation has recently been suggested to play an essential role in modulating neuronal Ca^{2+} channel function through regulation of the $Ca_v\beta3$ accessory subunit (Sandoval et al., 2006). Our findings raise the possibility that processing of the $Ca_v\alpha1$ protein may be affected in a similar way. To test this hypothesis, we used the web-based algorithm PESTfind (Rogers et al., 1986) in a search for potential $Ca_v\alpha1$ PEST sequences and found several putative motifs (amino acids 435–460, 807–820, 847–858, 1,732–1,745, and 1,839–1,865). Intriguingly, the highest scored potential PEST sequences obtained are highly conserved among species (Table I), with one located in the I–II linker of the $Ca_v\alpha1$ subunit and overlapping with the α1-interacting domain (AID), which is the primary binding region for $Ca_v\beta2$ (Fig. 7 A; Bodi et al., 2005). To determine whether these PEST sequences are involved in $Ca_v\alpha1$ degradation control, we generated two in-frame deletion mutants encompassing either the I–II ($Ca_v\alpha1$-ΔP) or II–III ($Ca_v\alpha1$-ΔH) cytosolic linker region (Fig. 7 A). Western blot and immunofluorescence analyses of serum-starved 293T cells transfected with these mutants revealed higher protein expression levels for both $Ca_v\alpha1$-ΔP and $Ca_v\alpha1$-ΔH mutants compared with $Ca_v\alpha1$-WT, which is consistent with the hypothesis that these motifs determine $Ca_v\alpha1$ protein stability (Fig. 7 B). Furthermore, a pulse-chase analysis, with a chase starting 36 h after cell starvation, revealed markedly increased protein stability of $Ca_v\alpha1$-ΔP and $Ca_v\alpha1$-ΔH compared with $Ca_v\alpha1$-WT (Fig. 7 C). In particular, $Ca_v\alpha1$-WT showed a short half-life typical of proteins containing PEST sequences (Dice, 1987), with a rapid and progressive degradation starting 4 h after the chase and reaching 50% of degradation 25 h after the chase. In contrast, $Ca_v\alpha1$-ΔP and $Ca_v\alpha1$-ΔH mutants were less sensitive to degradation and were degraded by only 23% and 15% after 25 h, respectively ($P < 0.001$). Notably, cotransfection of $Ca_v\beta2$-SE with $Ca_v\alpha1$-WT resulted in a considerable increase in the half-life of $Ca_v\alpha1$-WT (Fig. 7 C). In addition, transfection of 293T cells with $Ca_v\alpha1$ PEST sequences fused in frame with GFP resulted in marked instability of GFP, as shown by both Western blot and immunofluorescence analyses (Fig. 7 D), providing further evidence that these motifs are determinants for $Ca_v\alpha1$ protein stability. Consistent with the hypothesis that Akt-mediated protection of $Ca_v\alpha1$ degradation acts through PEST sequences, overexpression of AdAktDN or siAkt had no significant effect on protein levels of either $Ca_v\alpha1$-ΔP or $Ca_v\alpha1$-ΔH mutants (Fig. S4, B and C). To assess whether the observed PEST mechanism is caused by a direct Akt-dependent interaction between $Ca_v\beta2$ and $Ca_v\alpha1$, we performed in vitro binding assays using in vitro–translated [^{35}S]Met-labeled $Ca_v\alpha1$ cytosolic domains and a GST-fused $Ca_v\beta2$ C-terminal coiled-coil region. Notably, direct interaction took place between the Akt-phosphorylated $Ca_v\beta2$ C-terminal coiled-coil region and the $Ca_v\alpha1$ C-terminal domain (Fig. 7 E). No interactions were found with other $Ca_v\alpha1$ cytosolic domains (unpublished data), although it cannot be excluded that other binding sites may exist.

To assess whether PEST-deleted $Ca_v\alpha1$ channels are still functional, traffic appropriately to the membrane, and associate with the $Ca_v\beta2$ subunit, we measured Ca^{2+} current in $Ca_v\alpha1$-ΔH mutant–transfected cells. No significant differences in $I_{Ca,L}$ were found in cells transfected with $Ca_v\alpha1$-WT compared with $Ca_v\alpha1$-ΔH (Fig. 7 F). Conversely, although serum deprivation resulted in $I_{Ca,L}$ reduction in $Ca_v\alpha1$-WT–transfected cells, no significant changes were observed in $Ca_v\alpha1$-ΔH mutant–transfected cells (Fig. 7 F). This confirms that PEST-deleted $Ca_v\alpha1$-ΔH is resistant to rapid protein degradation and maintains its integrity and physiological function. Furthermore, current-voltage analysis (I-V curves) revealed that neither serum deprivation nor PEST-H deletion modifies steady-state activation parameters (Fig. S5). Also, all electrophysiological experiments were performed at a holding potential of −80 mV, which is a value far away from the potential for half steady-state inactivation (V0.5) of $I_{Ca,L}$, indicating that a change in the macroscopic current properties of $Ca_v1.2$ is unlikely.

Published March 23, 2009

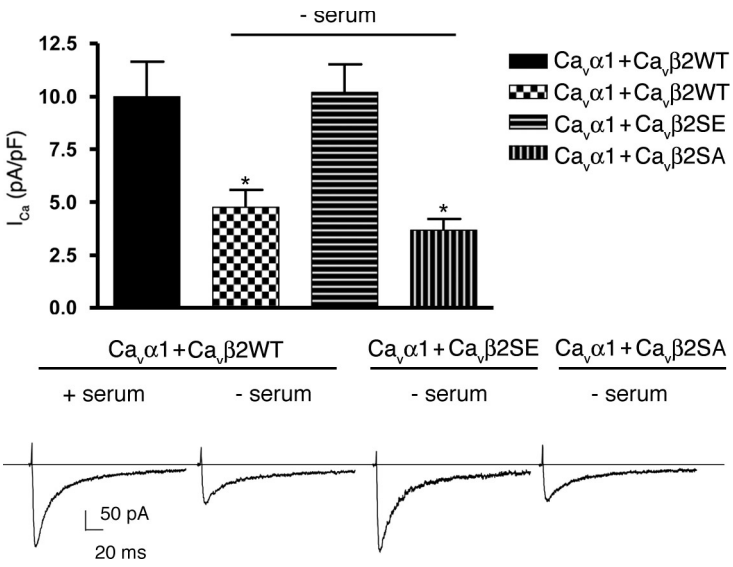

Figure 6. **Akt phosphorylation of $Ca_v\beta2$ preserves $Ca_v\alpha1$ currents.** Ca^{2+} currents recorded in cotransfected tsA-201 cells with YFP-$Ca_v\alpha1$ and $Ca_v\beta2$-WT, $Ca_v\beta2$-SE, or $Ca_v\beta2$-SA mutant cultivated for 36 h in the presence or absence of 10% fetal bovine serum. Currents were recorded 1–2 min after the whole cell configuration was achieved (i.e., after stabilization of the current) and were elicited by a 0-mV depolarization of 200-ms duration applied from a holding potential of −80 mV. Currents are normalized to cell capacitance (current density, picoampere/picofarad). Representative current traces are shown. $n > 35$ at each condition (*, $P < 0.05$ compared with YFP-$Ca_v\alpha1$; ANOVA). Error bars show SEM.

Collectively, our results suggest that Akt-mediated phosphorylation of $Ca_v\beta2$ regulates $Ca_v\alpha1$ density through protection of $Ca_v\alpha1$ PEST motifs from the cell protein degradation machinery. Impairment of this mechanism is expected to result in dysregulation of cardiomyocyte contractile function.

Discussion

This study reveals a mechanism through which the insulin IGF-1–PI3K–PDK1–Akt pathway can sustain or modulate Ca^{2+} entry in cardiac cells via the voltage-gated LTCC and eventually affect cardiac contractility. Using a mouse model with an inducible and cardiomyocyte-specific deletion of the upstream activator PDK1, we showed that Akt is of key importance for the structural organization and functionality of the LTCC complex at the plasma membrane. This regulation of LTCC activity is directly related to the Akt-mediated phosphorylation of the accessory subunit $Ca_v\beta2$, which in turn results in increased protein density of the pore-forming $Ca_v\alpha1$ subunit through protection of PEST sequences from the proteolytic degradation system. In the absence of phosphorylated Akt, the Ca^{2+} current is reduced, resulting in a decreased Ca^{2+} transient and contractility. Therefore, it is tempting to speculate that the Akt-mediated phosphorylation of $Ca_v\beta2$ and the consequent direct association of the $Ca_v\beta2$ C-terminal tail with the $Ca_v\alpha1$ C-terminal coiled-coil region (Fig. 7 E) may induce conformational changes that prevent PEST sequences from being recognized by the cell degradation system (Fig. 8). In addition, one cannot exclude the possibility that phosphorylated $Ca_v\beta2$ might also act indirectly through other, as of yet unknown, LTCC protein partners.

The identified mechanism alone is unlikely to be responsible for the detrimental cardiac defects observed in the PDK1 KO mouse model. To assess whether a reduction in the Akt antiapoptotic activity could lead to increased cell death, we measured caspase 3 activation (Fig. S1). However, consistent with previous evidence reported by Mora et al. (2003), our results failed to prove any significant involvement of this mechanism in the PDK1 KO phenotype. Our PDK1 KO mouse model does not appear to progress through slow transitional states, which are typical of heart failure, but rather progresses directly to a dilated cardiac phenotype, which eventually leads to premature

Table I. **PEST sequences are highly conserved in $Ca_v\alpha1$**

Species	Fragment	Sequences	PESTfind score
Mouse	PEST I	435-KGYLDWITQAEDIDPENEDEGMDEDK-460	8.45
Rat	PEST I	476-KGYLDWITQAEDIDPENEDEGMDEDK-501	8.45
Human	PEST I	446-KGYLDWITQAEDIDPENEDEGMDEEK-471	8.66
Mouse	PEST II	807-KSITADGESPPTTK-820	9.45
Rat	PEST II	848-KSITADGESPPTTK-861	9.45
Mouse	PEST III	837-HSNPDTAGEEDEEEPEMPVGPR-858	19.51
Rat	PEST III	878-HSNPDTAGEEDEEEPEMPVGPR-899	19.51
Human	PEST II	845-KSPYPNPETTGEEDEEEPEMPVGPR-869	20.26
Mouse	PEST IV	1,732-KTGNNQADTESPSH-1,745	5.5
Rat	PEST IV	1,772-KTGNNQADTESPSH-1,785	5.5
Mouse	PEST V	1,839-RMSEEAEYSEPSLLSTDMFSYQEDEH-1,865	5.86
Human	PEST IV	1,937-HDTEACSEPSLLSTEMLSYQDDENR-1,961	7.54
Human	PEST V	2,214-RGAPSEEELQDSR-2,226	7.71

Occurrence of PEST sites within the amino acid sequence of $Ca_v\alpha1$ from the mouse, rat, and human. Amino acid identity is underlined.

Published March 23, 2009

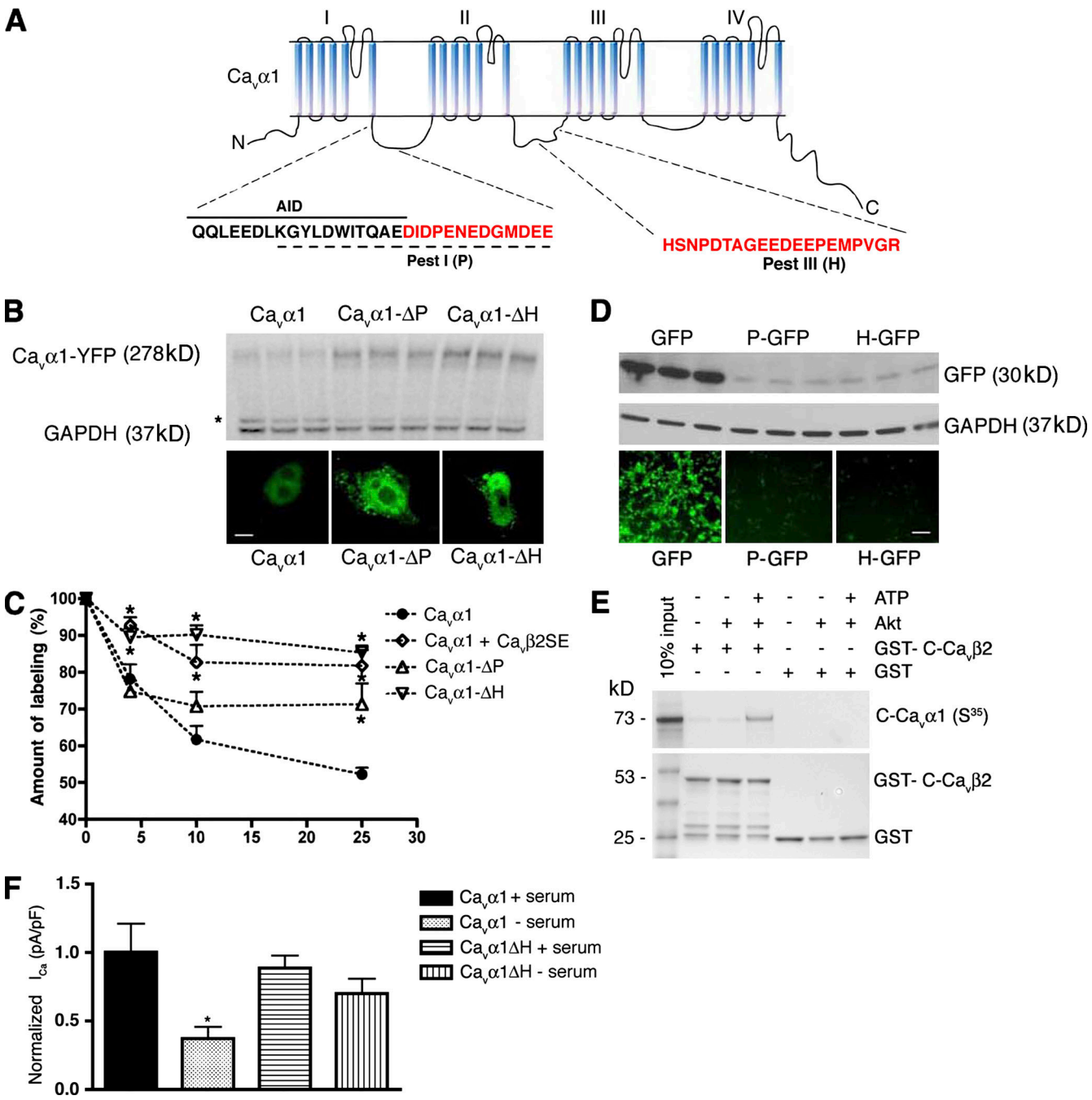

Figure 7. **Rapid protein degradation PEST sequences determine Ca$_v$α1 protein instability.** (A) Schematic representation of Ca$_v$α1 mapping the AID and PEST sequences in the I–II and II–III cytosolic loops. Deleted PEST sequences (P and H) are highlighted in red. (B) Western blot and immunofluorescence analyses showing relative levels of WT and PEST-deleted mutants of YFP-Ca$_v$α1 (n = 3). The asterisk indicates a YFP-Ca$_v$α1 degradation fragment. (C) Half-lives of WT Ca$_v$α1 subunit (alone or cotransfected with Ca$_v$β2-SE) and its in-frame ΔPEST mutants (Ca$_v$α1-ΔP and Ca$_v$α1-ΔH) were determined in COS-7 cells. After overnight starvation, transfected cells were pulse chased and analyzed along a time course (*, $P < 0.001$ compared with Ca$_v$α1; ANOVA; n = 3). Error bars show SD. (D) Western blot and immunofluorescence analyses showing relative levels of WT GFP and N-terminal fusion PEST mutants (n = 3). (E) The Ca$_v$α1 C terminus interacts with the Akt-phosphorylated GST-Ca$_v$β2 coiled-coil region. Bacterially expressed GST or GST-C-Ca$_v$β2 (Ca$_v$β2, amino acids 480–655) fusion protein and glutathione–Sepharose beads were incubated with equal amounts of in vitro–translated [^{35}S]Met-labeled C-Ca$_v$α1 (Ca$_v$α1, amino acids 1,477–2,169). Binding occurred only with Akt-phosphorylated GST-C-Ca$_v$β2. Bound proteins were resolved by SDS-PAGE (4–12%). 10% of the input protein in each binding reaction is shown. Coomassie staining of SDS-PAGE is shown in the bottom panel. (F) Ca^{2+} currents recorded in tsA-201 cells cotransfected with Ca$_v$β2-WT and either Ca$_v$α1-WT or Ca$_v$α1-ΔH and cultivated for 36 h in the presence or absence of 10% fetal bovine serum. Current densities (picoampere/picofarad) are normalized to the control condition. $n > 35$ at each condition (*, $P < 0.05$ compared with Ca$_v$α1; ANOVA). Error bars show SEM. Bars: (B) 5 µm; (D) 20 µm.

death (Fig. S1). Therefore, we hypothesize that the lethal phenotype is caused by activation of more complex systems that rapidly remodel the extracellular matrix and cell to cell contacts and change the energy metabolism. Further studies are required to unravel the complex mechanisms that contribute to the establishment of the observed PDK1 KO mouse heart phenotype.

Published March 23, 2009

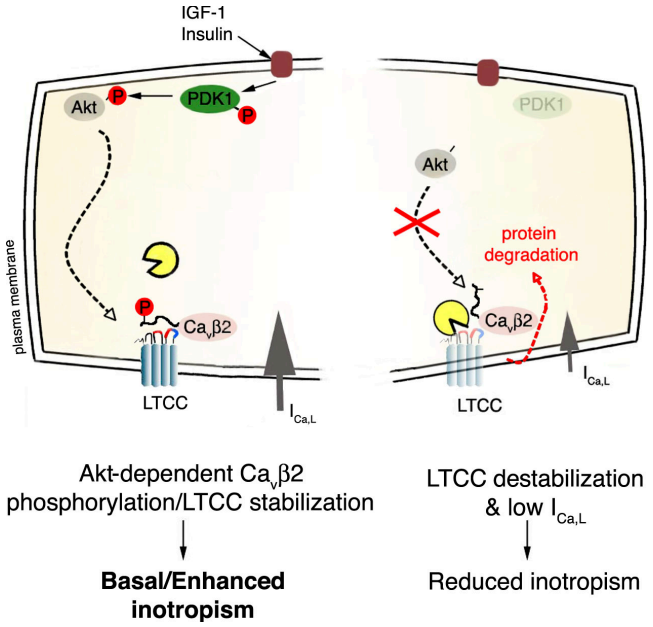

Figure 8. **Proposed mechanism.** Akt, followed by PDK1 activation, phosphorylates $Ca_v\beta2$ at the C-terminal coiled-coil domain. The phosphorylation allows association of the C-terminal portion of $Ca_v\beta2$ with the $Ca_v\alpha1$ C-terminal domain. In turn, a conformation shift prevents PEST sequence recognition, stabilizing $Ca_v\alpha1$ protein levels. The blue and red ribbons in $Ca_v\alpha1$ represent AID and PEST sequences, respectively.

Several findings have shown the importance of the insulin IGF-1–PI3K–Akt pathway in heart function. Our group has previously demonstrated that overexpression of an active form of Akt-1 results in improved cardiac inotropism both in vivo (Condorelli et al., 2002) and in vitro (Kim et al., 2003), augmenting $I_{Ca,L}$. Similar results were recently obtained in a mouse model with cardiac-specific Akt-1 nuclear overexpression (Rota et al., 2005) and in mice deficient for PTEN (phosphatase and tensin homologue deleted on chromosome 10), an antagonizer of PI3K activity (Sun et al., 2006). In addition, short-term administration of IGF-1 in animal experiments has also been reported to increase cardiac contractility (Duerr et al., 1995). However, the mechanism through which the insulin IGF-1–PI3K–Akt pathway affects Ca^{2+} current has remained elusive. In an elegant in vitro study, Viard et al. (2004) demonstrated that a region of the $Ca_v\beta2a$ subunit is involved in the PI3K-induced chaperoning of $Ca_v2.2\alpha$ in neurons. This PI3K-induced regulation was shown to be mediated by Akt phosphorylation of the $Ca_v\beta2a$ subunit, which in turn regulates $Ca_v2.2\alpha$ trafficking from the ER to the plasma membrane. Notably, the C-terminal region containing the putative Akt phosphorylation consensus site is conserved in all variants of the $Ca_v\beta2$ subunit both in neurons and the heart (Viard et al., 2004), thus illustrating the importance of this site. Interestingly, two very short human cardiac splice isoforms, $Ca_v\beta2f$ and $Ca_v\beta2g$, with preserved Akt sites have been shown to be essential for modulating Ca^{2+} channel function and $Ca_v\alpha1$ channel density (De Waard et al., 1994; Kobrinsky et al., 2005). Strikingly, the same two $Ca_v\beta2$ variants do not contain the PKA phosphorylation site (Kamp and Hell, 2000), which is consistent with our data suggesting no PKA involvement in the modulation of LTCC density (Fig. S2 B). As a corollary, the presence of this conserved C-terminal region in all $Ca_v\beta2$ splice isoforms corroborates the relevance of identifying new functional motifs that may give important insights into LTCC modulation. Consistent with an important functional role of the conserved $Ca_v\beta2$ C-terminal region, Lao et al. (2008) recently showed that, in the absence of the main $Ca_v\beta2$ protein domain, the selected C-terminal essential determinant is sufficient for $I_{Ca,L}$ stimulation. All together, this evidence supports the notion that this region is a potential pharmacological target.

In conclusion, we show that the insulin IGF-1–PI3K–PDK1–Akt pathway regulates $Ca_v\beta2$ chaperone activity through phosphorylation by Akt and suggest that, in turn, this controls $Ca_v\alpha1$ channel density by protection of $Ca_v\alpha1$ from PEST-dependent protein degradation (Fig. 8). This paradigm highlights an unanticipated regulatory function for Akt in modulating LTCC function and provides evidence for an essential role of Akt in the control of cardiomyocyte Ca^{2+} handling and contractility. Interestingly, the high level of conservation of PEST sequences in the $Ca_v\alpha1$ subunit throughout evolution (Table I) indicates that our proposed mechanism may play a universal role in regulating cell Ca^{2+} handling and survival. Because pathophysiological states are often accompanied by alterations in LTCC function (Mukherjee and Spinale, 1998), the elucidation of this novel regulatory pathway may open new therapeutic perspectives.

Materials and methods

Generation of genetically modified mice

Cardiac-specific PDK1-inducible KO mice (MerCreMer α-MHC PDK1) were generated by breeding $PDK1^{floxed/floxed}$ Tg mice (provided by D.R. Alessi, Medical Research Council Protein Phosphorylation Unit, University of Dundee, Dundee, Scotland, UK; Williams et al., 2000) with mice expressing the cardiac-specific MerCreMer α-MHC promoter-driven *cre* recombinase gene (provided by J.D. Molkentin, University of Cincinnati, Cincinnati, OH; Sohal et al., 2001). The resulting background strain of the MerCreMer mice was C57BL/6-SV129 and was unchanged throughout all experiments. Control animals used in this study were $PDK1^{floxed/floxed}$ littermates not expressing the *cre* recombinase gene and were treated with the same tamoxifen regiment. Tamoxifen dissolved in maize oil was injected intraperitoneally once a day at a dose of 75 mg/kg body weight. Male animals 7–8-wk old were used. All animal procedures were performed in accordance with the Guide for the Care and Use of Laboratory Animals and approved by the Institutional Animal Care and Use Committee.

Culture and treatment of mouse cardiomyocyte cells

Isolation of ventricular myocytes was performed as previously described (Care et al., 2007). Cells were infected with an adenovector expressing either no transgene (mock), HA–E40K-Akt (AdAkt), or Akt-K179M (AdAktDN) at MOI 100 and harvested 48 h after infection. The viral vector was amplified and purified in 3% sucrose/PBS by ViraQuest, Inc.

Cell culture and cDNA mutagenesis

Cell transfection was performed in serum-starved medium using Lipofectamine 2000 (Invitrogen) according to the manufacturer's instructions. 5 µM Akt-XI inhibitor (EMD), insulin (Sigma-Aldrich), 1 µM bafilomycin-A1 (Sigma-Aldrich), 25 µM MG132 (EMD), and 25 µM calpeptin (EMD) were used as described in Results. *Cacnb2* cDNA (complete coding sequence, cDNA clone MGC:129335, IMAGE:40047531; American Type Culture Collection) was cloned in the pcDNA3 vector. Site-directed mutagenesis was performed using the QuikChange Site-Directed Mutagenesis kit (Agilent Technologies). $Ca_v\alpha1$ PEST deletion mutants and GFP fusion proteins were generated by PCR. YFP-$Ca_v\alpha1$ expression plasmids were provided by N. Soldatov (National Institute on Aging, National Institutes of Health, Baltimore, MD). A lentivirus vector was generated and used as an expression vector for siRNA-mediated silencing of the *akt* gene (siAkt). The sequence used (5′-TGCCCTTCTACAACCAGGATT-3′) was chosen in a conserved region between rat, mouse, and human and has been validated for targeting Akt-1 and -2 (Katome et al., 2003). All constructs were confirmed by DNA sequencing.

Published March 23, 2009

Ca^{2+} current measurement

Macroscopic $I_{Ca,L}$ was recorded at room temperature (~22°C) using the whole cell patch-clamp technique in native cells as previously described (Maier et al., 2003; Aimond et al., 2005). External recording solution contained 136 mM tetraethylammonium (TEA)-Cl, 2 mM $CaCl_2$, 1.8 mM $MgCl_2$, 10 mM Hepes, 5 mM 4-aminopyridine, and 10 mM glucose, pH 7.4, with TEA-OH. Pipette solution contained 125 mM CsCl, 20 mM TEA-Cl, 10 mM EGTA, 10 mM Hepes, 5 mM phosphocreatine, 5 mM Mg_2-ATP, and 0.3 GTP, pH 7.2, with CsOH. Myocytes were held at −80 mV, and 10-mV depolarizing steps from −50 to 50 mV for 300 ms were applied. Analysis was performed using a microscope (Diaphot 200; Nikon) equipped with 10× NA 20 objective lenses (CFWN; Nikon). pCLAMP 9 (MDS Analytical Technologies) was used as acquisition software. For electrophysiological recordings of recombinant $Ca_v\alpha1$ currents, tsA-201 cells were transfected in OptiMEM (Invitrogen) with a DNA mix containing plasmids encoding YFP-$Ca_v\alpha1$, $Ca_v\beta2$ subunit (either $Ca_v\beta2$-WT, $Ca_v\beta2$-SE, or $Ca_v\beta2$-SA), $Ca_v\alpha2\delta1$ subunit, and CD8 (in a ratio of 1:2:0.5:0.1). After 24 h, cells were cultured in DME with or without serum for 36 h, and electrophysiological recordings were performed on cells expressing both YFP-$Ca_v\alpha1$ and CD8, which is identified using anti-CD8–coated beads (Dynabeads; Invitrogen). The ~330-mosM extracellular solution contained 135 mM NaCl, 20 mM TEA-Cl, 5 mM $CaCl_2$, 1 $MgCl_2$, and 10 mM Hepes (pH adjusted to 7.4 with KOH). Borosilicate glass pipettes have a typical resistance of 1.5–3 MW when filled with an ~315-mosM internal solution containing 140 mM CsCl, 10 mM EGTA, 10 mM Hepes, 3 mM Mg-ATP, 0.6 mM GTP-Na, and 2 mM $CaCl_2$ (pH adjusted to 7.2 with KOH). Analysis was performed using a microscope (x71; Olympus). Data acquisition was performed with pCLAMP 9 software.

Fluorescent measurement of $[Ca^{2+}]_i$

Isolated myocytes were loaded with 5 µM Fura-PE3 acetoxymethyl (TefLabs) and analyzed as previously described (Bassani et al., 1994; DeSantiago et al., 2002). Analysis was performed using a Diaphot 200 microscope. Data acquisition and analysis were performed using pCLAMP software (Clampex and Clampfit version 8.2; MDS Analytical Technologies).

Akt and PKC kinase assay

Myocardial tissue lysates were tested using the Akt Kinase Assay kit (Cell Signaling Technology) and PKC (Millipore) according to the manufacturer's instructions.

Western blot analysis and antibodies

Protein expression was evaluated in total lysates or cell fractions by Western blot analysis according to standard procedures. Antibodies against the following proteins were used: $Ca_v\alpha1$ (Novus Biologicals); $Ca_v\alpha1$ and $Ca_v\beta2$ (provided by H. Haase, Max Delbrück Center for Molecular Medicine, Berlin, Germany); Ryr and Ryr2-P2809 (provided by A. Marks, Columbia University, New York, NY); PDK1 (EMD); Akt-1, -2, and -3, Akt, Akt-P308, and anti–phospho-Ser/Thr-Akt substrate (Cell Signaling Technology); PLN and PLN-P16 (Novus Biologicals); calsequestrin (BD); caspase 3 (Cell Signaling Technology); HA (Roche); GFP/YFP (GeneTex, Inc.); tubulin (Novus Biologicals); GSK-3β (Cell Signaling Technology); and glyceraldehyde-3-phosphate dehydrogenase (GAPDH; Cell Signaling Technology). ImageJ software (National Institutes of Health) was used to perform densitometry analyses.

Tissue preparation, immunoprecipitation, and in vitro phosphorylation

When described, overnight-fasted mice were injected intraperitoneally with 1 mU/g insulin or saline solution. 20 min after injection, the hearts were rapidly extracted, freeze clamped in liquid nitrogen, and homogenized to a powder in liquid nitrogen. In vitro phosphorylation assays on immunoprecipitates were performed as described previously (Haase et al., 1999).

Cell fractionation

Pulverized hearts were homogenized in ice-cold solution 1 (300 mM sucrose, 10 mM Tris-HCl, pH 7.5, 1 mM EDTA, 1 mM EGTA, 50 mM NaF, 1 mM Na_3VO_4, and protease inhibitors) at 1.5 ml/ventricle by three bursts of 10 s in a homogenizer (PT 3000; Polytron). Homogenates were then incubated for 15 min on ice (whole homogenates). Samples were spun at 1,000 *g* for 10 min at 4°C. Pellets were washed in solution 1 and spun at 1,000 *g* for 10 min at 4°C, and supernatants were filtered through four layers of cheese cloth and centrifuged at 10,000 *g* for 30 min at 4°C. Supernatants were then centrifuged at 143,000 *g* for 30 min at 4°C, and pellets were resuspended in solution 2 (600 mM KCl, 30 mM Tris-HCl, pH 7.5, 300 mM sucrose, 1 mM EDTA, 1 mM EGTA, 50 mM NaF, 1 mM Na_3VO_4, and protease inhibitors). Supernatants were saved as cytosolic fractions. Resuspended pellets from a further centrifugation at 143,000 *g* for 45 min at 4°C were resuspended in solution 3 (100 mM KCl, 20 mM Tris-HCl, pH 7.5, 300 mM sucrose, 1 mM EDTA, 1 mM EGTA, 50 mM NaF, 1 mM Na_3VO_4, and protease inhibitors) and saved as ER fractions. All aliquots were stored at −80°C.

Histology and confocal microscopy

Fixation, staining, and confocal analysis were performed as previously described (Care et al., 2007). Confocal microscopy was performed using a confocal microscope (Radiance 2000; Bio-Rad Laboratories) with a 60× Plan-Apochromat NA 1.4 objective (Carl Zeiss, Inc.). Individual images (1,024 × 1,024 pixels) were converted to tiff format and merged as pseudocolor RGB images using Imaris (Bitplane AG).

Pulse-chase and immunoprecipitation experiments

36 h after transfection, 293T cells were starved for 30 min in Met- and Cys-free DME (Sigma-Aldrich) and were then labeled for 30 min by adding 500 µCi ^{35}S-labeled L-Met and 2 mM L-Cys. Radioactive media was eventually washed out with PBS (time 0 pulse) and replaced with normal DME. Time points were at 4, 10, and 25 h after pulse. Anti-GFP polyclonal IgG (GTX20290) was used for immunoprecipitation. Radioactivity was quantitated with ImageQuant 5.2 software (GE Healthcare).

GST pull-down assay

Affinity-purified GST fusion proteins were generated using a pGEX system (GE Healthcare) and phosphorylated as described below. GST fusion protein bound to glutathione–Sepharose 4B beads (GE Healthcare) was incubated with 25 µl of ^{35}S-labeled Met protein with moderate shaking at 25°C for 2 h in 200 µl of binding buffer containing 20 mM Hepes, pH 7.9, 1 mM EDTA, 10% glycerol, 0.15 M KCl, 0.05% Nonidet P-40, and 1 mM DTT. ^{35}S-labeled probes were generated from the C-terminal region of $Ca_v\alpha1$ cDNA fragments under control of the T7 promoter using the TnT Quick Coupled Reticulocyte Lysate System (L1170; Promega), washed three times with washing buffer (20 mM Hepes, pH 7.9, 1 mM EDTA, 10% glycerol, 250 mM KCl, and 0.1% Nonidet P-40), and centrifuged. Bound proteins were eluted in SDS sample buffer, subjected to SDS-PAGE, and detected by autoradiography. Recombinant GST-$Ca_v\beta2$ beads or GST beads were phosphorylated by incubation with recombinant Akt (Millipore). In brief, 5 µg GST-$Ca_v\beta2$ or GST beads were incubated at 30°C for 45 min in a 50-µl solution containing 2 µg activated Akt kinase, 10 mM Hepes-KOH, pH 7.5, 50 mM γ-glycerophosphate, 50 mM NaCl, 1 mM dithiothreitol, 10 mM $MnCl_2$, and 1 mM ATP.

Statistical analysis

Statistical comparison was performed within at least three independent experiments by paired or unpaired Student's *t* test, whereas comparison between groups was analyzed by one-way repeated-measures analysis of variance (ANOVA) combined with a Newman-Keuls post-test to compare different values using Prism 4.0 software (GraphPad Software, Inc.). Differences with $P < 0.05$ were considered statistically significant.

Online supplemental material

Fig. S1 shows additional biochemical, histological, and echocardiographic analyses of mice lacking PDK1 expression. Fig. S2 shows SERCA2 level and phosphorylation of specific PKA regulatory sites in two SR Ca^{2+} regulatory proteins, Ryr (Ryr2-P2809) and PLN (PLN-P16). Fig. S3 shows representative Ca^{2+} traces and twitch Ca^{2+} transient amplitude in KO compared with WT cardiomyocytes. Fig. S4 shows coimmunoprecipitation of $Ca_v\beta2$ with insulin-activated Akt isoforms and the effects of dominant-active and -negative Akt as well as siAkt on the $Ca_v\alpha1$ protein level. Fig. S5 shows current-voltage analysis (I-V curves) of cells transfected with $Ca_v\alpha1$-WT or $Ca_v\alpha1$-ΔH in normal or serum-free conditions. Table S1 shows echocardiography analysis values of WT and KO mice. Online supplemental material is available at http://www.jcb.org/cgi/content/full/jcb.200805063/DC1.

We thank Dr. Dario R. Alessi for PDK1$^{floxed/floxed}$ Tg mice, Dr. Jeffrey D. Molkentin for MerCreMer α-MHC mice, Dr. Hannelore Haase for $Ca_v\alpha1$ and $Ca_v\beta2$ antibodies, Dr. Nikolai Soldatov for YFP-$Ca_v\alpha1$, and Dr. Marie-Louise Bang for critical comments on the manuscript.

This work was sponsored by grants from the National Institutes of Health (HL078797-01A1 to G. Condorelli, HL28143 to J.H. Brown, and HL080101 to J.H. Brown and D.M. Bers), the Marie Curie Outgoing Research Fellowship European Union Sixth Framework Program (8566 to D. Catalucci), the Perlman Fund for Cardiovascular Research and Education, and the San Diego Foundation for Cardiovascular Research and Education (grant to K.L. Peterson). S. Richard holds a permanent position as Centre National de la Recherche Scientifique Director of Research.

Submitted: 13 May 2008
Accepted: 23 February 2009

Published March 23, 2009

References

Aimond, F., S.P. Kwak, K.J. Rhodes, and J.M. Nerbonne. 2005. Accessory Kvbeta1 subunits differentially modulate the functional expression of voltage-gated K+ channels in mouse ventricular myocytes. *Circ. Res.* 96:451–458.

Bassani, J.W., R.A. Bassani, and D.M. Bers. 1994. Relaxation in rabbit and rat cardiac cells: species-dependent differences in cellular mechanisms. *J. Physiol.* 476:279–293.

Bayascas, J.R., S. Wullschleger, K. Sakamoto, J.M. Garcia-Martinez, C. Clacher, D. Komander, D.M. van Aalten, K.M. Boini, F. Lang, C. Lipina, et al. 2008. Mutation of PDK1 PH domain inhibits PKB/Akt leading to small size and insulin-resistance. *Mol. Cell. Biol.* 28:3258–3272.

Belles, B., J. Hescheler, W. Trautwein, K. Blomgren, and J.O. Karlsson. 1988. A possible physiological role of the Ca-dependent protease calpain and its inhibitor calpastatin on the Ca current in guinea pig myocytes. *Pflugers Arch.* 412:554–556.

Bers, D.M. 2002. Cardiac excitation-contraction coupling. *Nature*. 415:198–205.

Bers, D.M., and E. Perez-Reyes. 1999. Ca channels in cardiac myocytes: structure and function in Ca influx and intracellular Ca release. *Cardiovasc. Res.* 42:339–360.

Blair, L.A., K.K. Bence-Hanulec, S. Mehta, T. Franke, D. Kaplan, and J. Marshall. 1999. Akt-dependent potentiation of L channels by insulin-like growth factor-1 is required for neuronal survival. *J. Neurosci.* 19:1940–1951.

Bodi, I., G. Mikala, S.E. Koch, S.A. Akhter, and A. Schwartz. 2005. The L-type calcium channel in the heart: the beat goes on. *J. Clin. Invest.* 115:3306–3317.

Bourinet, E., M.E. Mangoni, and J. Nargeot. 2004. Dissecting the functional role of different isoforms of the L-type Ca2+ channel. *J. Clin. Invest.* 113:1382–1384.

Care, A., D. Catalucci, F. Felicetti, D. Bonci, A. Addario, P. Gallo, M.L. Bang, P. Segnalini, Y. Gu, N.D. Dalton, et al. 2007. MicroRNA-133 controls cardiac hypertrophy. *Nat. Med.* 13:613–618.

Catalucci, D., and G. Condorelli. 2006. Effects of Akt on cardiac myocytes: location counts. *Circ. Res.* 99:339–341.

Catterall, W.A. 2000. Structure and regulation of voltage-gated Ca2+ channels. *Annu. Rev. Cell Dev. Biol.* 16:521–555.

Ceci, M., J. Ross Jr., and G. Condorelli. 2004. Molecular determinants of the physiological adaptation to stress in the cardiomyocyte: a focus on AKT. *J. Mol. Cell. Cardiol.* 37:905–912.

Condorelli, G., A. Drusco, G. Stassi, A. Bellacosa, R. Roncarati, G. Iaccarino, M.A. Russo, Y. Gu, C. Chung, M. Latronico, et al. 2002. Akt induces enhanced myocardial contractility and cell size in vivo in transgenic mice. *Proc. Natl. Acad. Sci. USA*. 99:12333–12338.

De Waard, M., D.R. Witcher, and K.P. Campbell. 1994. Functional properties of the purified N-type Ca2+ channel from rabbit brain. *J. Biol. Chem.* 269:6716–6724.

DeSantiago, J., L.S. Maier, and D.M. Bers. 2002. Frequency-dependent acceleration of relaxation in the heart depends on CaMKII, but not phospholamban. *J. Mol. Cell. Cardiol.* 34:975–984.

Dice, J.F. 1987. Molecular determinants of protein half-lives in eukaryotic cells. *FASEB J.* 1:349–357.

Duerr, R.L., S. Huang, H.R. Miraliakbar, R. Clark, K.R. Chien, and J. Ross Jr. 1995. Insulin-like growth factor-1 enhances ventricular hypertrophy and function during the onset of experimental cardiac failure. *J. Clin. Invest.* 95:619–627.

Haase, H., T. Podzuweit, G. Lutsch, A. Hohaus, S. Kostka, C. Lindschau, M. Kott, R. Kraft, and I. Morano. 1999. Signaling from beta-adrenoceptor to L-type calcium channel: identification of a novel cardiac protein kinase A target possessing similarities to AHNAK. *FASEB J.* 13:2161–2172.

Kamp, T.J., and J.W. Hell. 2000. Regulation of cardiac L-type calcium channels by protein kinase A and protein kinase C. *Circ. Res.* 87:1095–1102.

Katome, T., T. Obata, R. Matsushima, N. Masuyama, L.C. Cantley, Y. Gotoh, K. Kishi, H. Shiota, and Y. Ebina. 2003. Use of RNA interference-mediated gene silencing and adenoviral overexpression to elucidate the roles of AKT/protein kinase B isoforms in insulin actions. *J. Biol. Chem.* 278:28312–28323.

Kim, Y.K., S.J. Kim, A. Yatani, Y. Huang, G. Castelli, D.E. Vatner, J. Liu, Q. Zhang, G. Diaz, R. Zieba, et al. 2003. Mechanism of enhanced cardiac function in mice with hypertrophy induced by overexpressed Akt. *J. Biol. Chem.* 278:47622–47628.

Kobrinsky, E., S. Tiwari, V.A. Maltsev, J.B. Harry, E. Lakatta, D.R. Abernethy, and N.M. Soldatov. 2005. Differential role of the alpha1C subunit tails in regulation of the Cav1.2 channel by membrane potential, beta subunits, and Ca2+ ions. *J. Biol. Chem.* 280:12474–12485.

Krappmann, D., F.G. Wulczyn, and C. Scheidereit. 1996. Different mechanisms control signal-induced degradation and basal turnover of the NF-kappaB inhibitor IkappaB alpha in vivo. *EMBO J.* 15:6716–6726.

Lao, Q.Z., E. Kobrinsky, J.B. Harry, A. Ravindran, and N.M. Soldatov. 2008. New determinant for the CaVbeta2 subunit modulation of the CaV1.2 calcium channel. *J. Biol. Chem.* 283:15577–15588.

Lawlor, M.A., A. Mora, P.R. Ashby, M.R. Williams, V. Murray-Tait, L. Malone, A.R. Prescott, J.M. Lucocq, and D.R. Alessi. 2002. Essential role of PDK1 in regulating cell size and development in mice. *EMBO J.* 21:3728–3738.

Maier, L.S., T. Zhang, L. Chen, J. DeSantiago, J.H. Brown, and D.M. Bers. 2003. Transgenic CaMKIIdeltaC overexpression uniquely alters cardiac myocyte Ca2+ handling: reduced SR Ca2+ load and activated SR Ca2+ release. *Circ. Res.* 92:904–911.

McMullen, J.R., T. Shioi, L. Zhang, O. Tarnavski, M.C. Sherwood, P.M. Kang, and S. Izumo. 2003. Phosphoinositide 3-kinase(p110alpha) plays a critical role for the induction of physiological, but not pathological, cardiac hypertrophy. *Proc. Natl. Acad. Sci. USA*. 100:12355–12360.

McMullen, J.R., T. Shioi, W.Y. Huang, L. Zhang, O. Tarnavski, E. Bisping, M. Schinke, S. Kong, M.C. Sherwood, J. Brown, et al. 2004. The insulin-like growth factor 1 receptor induces physiological heart growth via the phosphoinositide 3-kinase(p110alpha) pathway. *J. Biol. Chem.* 279:4782–4793.

Mora, A., A.M. Davies, L. Bertrand, I. Sharif, G.R. Budas, S. Jovanovic, V. Mouton, C.R. Kahn, J.M. Lucocq, G.A. Gray, et al. 2003. Deficiency of PDK1 in cardiac muscle results in heart failure and increased sensitivity to hypoxia. *EMBO J.* 22:4666–4676.

Mora, A., D. Komander, D.M. van Aalten, and D.R. Alessi. 2004. PDK1, the master regulator of AGC kinase signal transduction. *Semin. Cell Dev. Biol.* 15:161–170.

Mukherjee, R., and F.G. Spinale. 1998. L-type calcium channel abundance and function with cardiac hypertrophy and failure: a review. *J. Mol. Cell. Cardiol.* 30:1899–1916.

Pereira, L., J. Matthes, I. Schuster, H.H. Valdivia, S. Herzig, S. Richard, and A.M. Gomez. 2006. Mechanisms of [Ca2+]i transient decrease in cardiomyopathy of db/db type 2 diabetic mice. *Diabetes*. 55:608–615.

Quignard, J.F., M.C. Harricane, C. Menard, P. Lory, J. Nargeot, L. Capron, D. Mornet, and S. Richard. 2001. Transient down-regulation of L-type Ca(2+) channel and dystrophin expression after balloon injury in rat aortic cells. *Cardiovasc. Res.* 49:177–188.

Rechsteiner, M. 1990. PEST sequences are signals for rapid intracellular proteolysis. *Semin. Cell Biol.* 1:433–440.

Richard, S., E. Perrier, J. Fauconnier, R. Perrier, L. Pereira, A.M. Gomez, and J.P. Benitah. 2006. 'Ca(2+)-induced Ca(2+) entry' or how the L-type Ca(2+) channel remodels its own signalling pathway in cardiac cells. *Prog. Biophys. Mol. Biol.* 90:118–135.

Rogers, S., R. Wells, and M. Rechsteiner. 1986. Amino acid sequences common to rapidly degraded proteins: the PEST hypothesis. *Science*. 234:364–368.

Romanin, C., P. Grosswagen, and H. Schindler. 1991. Calpastatin and nucleotides stabilize cardiac calcium channel activity in excised patches. *Pflugers Arch.* 418:86–92.

Rota, M., A. Boni, K. Urbanek, E. Padin-Iruegas, T.J. Kajstura, G. Fiore, H. Kubo, E.H. Sonnenblick, E. Musso, S.R. Houser, et al. 2005. Nuclear targeting of Akt enhances ventricular function and myocyte contractility. *Circ. Res.* 97:1332–1341.

Sandoval, A., N. Oviedo, A. Tadmouri, T. Avila, M. De Waard, and R. Felix. 2006. Two PEST-like motifs regulate Ca2+/calpain-mediated cleavage of the CaVbeta3 subunit and provide important determinants for neuronal Ca2+ channel activity. *Eur. J. Neurosci.* 23:2311–2320.

Smith, L.K., M. Bradshaw, D.E. Croall, and C.W. Garner. 1993. The insulin receptor substrate (IRS-1) is a PEST protein that is susceptible to calpain degradation in vitro. *Biochem. Biophys. Res. Commun.* 196:767–772.

Sohal, D.S., M. Nghiem, M.A. Crackower, S.A. Witt, T.R. Kimball, K.M. Tymitz, J.M. Penninger, and J.D. Molkentin. 2001. Temporally regulated and tissue-specific gene manipulations in the adult and embryonic heart using a tamoxifen-inducible Cre protein. *Circ. Res.* 89:20–25.

Sun, H., B.G. Kerfant, D. Zhao, M.G. Trivieri, G.Y. Oudit, J.M. Penninger, and P.H. Backx. 2006. Insulin-like growth factor-1 and PTEN deletion enhance cardiac L-type Ca2+ currents via increased PI3Kalpha/PKB signaling. *Circ. Res.* 98:1390–1397.

Viard, P., A.J. Butcher, G. Halet, A. Davies, B. Nurnberg, F. Heblich, and A.C. Dolphin. 2004. PI3K promotes voltage-dependent calcium channel trafficking to the plasma membrane. *Nat. Neurosci.* 7:939–946.

Williams, M.R., J.S. Arthur, A. Balendran, J. van der Kaay, V. Poli, P. Cohen, and D.R. Alessi. 2000. The role of 3-phosphoinositide-dependent protein kinase 1 in activating AGC kinases defined in embryonic stem cells. *Curr. Biol.* 10:439–448.

Yamaguchi, H., M. Hara, M. Strobeck, K. Fukasawa, A. Schwartz, and G. Varadi. 1998. Multiple modulation pathways of calcium channel activity by a beta subunit. Direct evidence of beta subunit participation in membrane trafficking of the alpha1C subunit. *J. Biol. Chem.* 273:19348–19356.